

# Evaluation on Curing Properties and Kinetics of Isophthalonitrile Oxide

Yaqin Fan<sup>1</sup>, Chunlan Tang<sup>1</sup>, Qing Hu<sup>2</sup>, Yonglin Lei<sup>1\*</sup>, Jichuan Huo<sup>1</sup>

<sup>1</sup>Southwest University of Science and Technology, School of Materials Science and Engineering, Mianyang, 621010, People's Republic of China

<sup>2</sup>Yixing Danson Science & Technology Co., Ltd., Yixing, 214200, People's Republic of China

\*Corresponding author: e-mail: leiyonglin@163.com

N,N-dihydroxybenzene-1,3-dicarboximidoyl dichloride was synthesized from benzene-1,3-dicarboxaldehyde and characterized by fourier transform infrared spectroscopy (FT-IR) and nuclear magnetic resonance (<sup>1</sup>H and <sup>13</sup>C NMR). The elastomer was prepared through the 1,3-dipolar cycloaddition of reaction between liquid polybutadiene (LPB) and isophthalonitrile oxide in this work. The tensile strength of different elastomer was enhanced from 0.14 MPa to 0.33 MPa as the elongation at break decreased from 145% to 73%, and the modulus increased from 0.09 kPa to 0.47 kPa. The parameters of kinetic indicated that the curing reaction was first order reaction and the apparent activation energy of each curing system was less than 10.10 kJ/mol when the content of N,N-dihydroxybenzene-1,3-dicarboximidoyl dichloride was increased from 7% to 12%. These results suggested that nitrile oxides achieved curing of polymer binders at room temperature and this work had definite guiding significance for the application of nitrile oxides in polymer binders.

**Keywords:** N,N-dihydroxybenzene-1,3-dicarboximidoyl dichloride; kinetics; elastomer; synthesis; 1,3-dipolar cycloaddition.

## INTRODUCTION

Polymers binder as a binder in the composite solid propellants is generally accepted, such as polyurethane, glycidyl azide polymers and hydroxyl-terminated polymers<sup>1-3</sup>. The necessary mechanical properties and structural integrity of composite solid propellants are required by polymer binders<sup>4</sup>. In recent years, the polymer/isocyanate curing system has been extensively used in composite solid propellant. The curing system has some problems of high curing temperature, greater shrinkage stress during curing, depending, cracking and other defects in the cured product<sup>5</sup>. Hence, there is another type of non-isocyanate adhesive curing technology to solve the polymer/isocyanate curing system of problems<sup>6</sup>. Non-isocyanate adhesive curing technology has unique advantages of good environmental adaptability, low toxicity, excellent performance, easy formability, compatible with ammonium dinitramide (ADN) and low-cost.

Non-isocyanate adhesive curing technology is a 1,3-dipolar cycloaddition of reaction which can achieve polymer adhesive curing, reduce the curing temperature, improve the properties of composite solid propellants, form non-volatile component and stay in the curing system<sup>7-11</sup>. Nitrile oxide holds the highest activity in the 1,3-dipolar cycloaddition reaction, usually containing RC≡NO structure<sup>12</sup>. Its functional group -CNO has highly polarized C-N and N-O, which are capable of reacting with the unsaturated bond (C=C, C≡C) through the 1,3-dipolar cycloaddition reaction. Nitrile oxide has a higher curing activity than azide group, which is almost cured at room or lower temperature.

Polyfunctional nitrile oxides were designed by the researcher, which had low-activity, as the precursor to achieve unsaturated ethylene structural polymers curing, but the mechanical properties of the prepared elastomer were poor<sup>13</sup>. Highly active nitrile oxide can make the curing reaction more complete and has better curing effect in the work<sup>14-17</sup>. Herein, LPB was considered as the matrix, the synthesized N,N-dihydroxybenzene-1,3-

-dicarboximidoyl dichloride as the precursor reacted with triethylamine to prepare highly active nitrile oxides, and the LPB was cured at room temperature. The mechanical properties, shore hardness, thermal properties and surface properties of elastomer were studied under different curing ratios. Kinetics research was used to explain and optimize the curing reaction process. These researches will have some theoretical and practical implications for the application of nitrile oxides in polymer binders.

## EXPERIMENTAL

### Material

Benzene-1,3-dicarboxaldehyde (98%) and N-chlorosuccinimide (98%, NCS) were purchased from Shanghai Macklin Biochemical Co., Ltd. Hydroxylamine hydrochloride, N,N-dimethylformamide (DMF), triethylamine (Et<sub>3</sub>N), dichloromethane (CH<sub>2</sub>Cl<sub>2</sub>), sodium hydroxide (NaOH) and ethanol (EtOH) were obtained from Kelong chemical reagent factory (Chengdu China). Liquid polybutadiene rubber (LPB), M<sub>n</sub> = 3000 g/mol, was supplied by Sigma-Aldrich Co., Ltd. All the chemicals were used without further purification.

### Characterizations

An FT-IR spectrophotometer (PE, Nicolet5700, America) was used in recording the IR spectra of compounds and the polybutadiene elastomers. The infrared spectra (FT-IR) of the samples were scanned from 4000 cm<sup>-1</sup> to 400 cm<sup>-1</sup>, with a resolution superior to 0.5 cm<sup>-1</sup>. <sup>1</sup>H NMR and <sup>13</sup>C NMR spectra were recorded on a 600 MHz NMR spectrometer (Bruker, Avance600, Switzerland) with DMSO-d<sub>6</sub> as solvent. The mass spectrographic analysis of the compound was carried out with LC/MS instrument (Varian, 1200L, America) with an ESI source. The melting point of compounds was tested by melting point instrument (Kehang, Ry-1G, China). The components of the compounds were determined by elementary analysis (Elementar, Vario ELCUBE, Germany).

According to GB/T 528-2009 (China) "Rubber, vulcanized or thermoplastic-determination of tensile stress-strain properties", the tensile stress and the elongation at break of the elastomers were measured by putting the dumbbell-shaped sample (size:  $100 \times 8 \times 2 \text{ mm}^3$ ) on the temperature controlled electronic universal material testing machine (MTS, C45.504, China). The stress-strain measurements were performed at  $25^\circ\text{C}$  and the stretching rate was  $100 \text{ mm/min}$ .

Based on the GB/T 6031-1998 (China) "Rubber, vulcanized or thermoplastic-Determination of hardness", shore hardness of the elastomers were investigated by a shore durometer. Each sample was measured for five times and the results were averaged.

Thermogravimetric analysis of the elastomers was carried out using TGA instrument (SDT, Q600, TA company, America) under nitrogen atmosphere flow of  $100 \text{ mL/min}$  by increasing the temperature from  $25^\circ\text{C}$  to  $800^\circ\text{C}$  at  $10^\circ\text{C/min}$ .

The thermal properties of the elastomers were characterized by differential scanning calorimetry (DSC, Q2000, TA company, America) under nitrogen atmosphere flow of  $100 \text{ mL/min}$  by increasing the temperature from  $-90^\circ\text{C}$  to  $50^\circ\text{C}$  at  $10^\circ\text{C/min}$ . The glass transition temperature ( $T_g$ ) was determined from the scan.

Static contact angle measurements were carried out on a contact angle measuring instrument (Kruss, DSA30, Germany) by depositing a drop of water on the surface of the elastomer (size:  $80 \times 10 \times 5 \text{ mm}^3$ ). Each sample was tested at least three times and the results were averaged.

A field emission scanning electron microscope (FE-SEM) image of the fracture surface of the elastomers were obtained on a Zeiss Ultra 55 scanning electron microscope (SEM) with an accelerating voltage of  $15 \text{ kV}$ .

Differential scanning calorimetry analysis was carried out under nitrogen flow rate of  $50 \text{ mL/min}$  to evaluate the effects of curing agent at different heating rates ( $b = 5, 10, 15, 20$  and  $25^\circ\text{C/min}$ ) to calculate the kinetic parameters of the curing system by using DSC analyzer Q2000 (TA company, America).

### Synthesis of benzene-1,3-dicarboxaldehyde dioxime<sup>18</sup>

A solid of hydroxylamine hydrochloride ( $0.24 \text{ mol}$ ) was added to a solution of benzene-1,3-dicarboxaldehyde ( $0.1 \text{ mol}$ ) in ethanol ( $17 \text{ mL}$ ) with stirring at reflux. Sodium hydroxide ( $0.22 \text{ mol}$ ) was added to the reaction solution followed by the sodium chloride was precipitated. After being stirred for  $3 \text{ h}$  at  $78^\circ\text{C}$ , the solvent was removed by evaporation, and the reaction mixture was repeatedly washed with water and dried in vacuum to a constant weight. Finally, recrystallization from ethanol yielded a light yellow solid ( $13.97 \text{ g}$ ), and the yield was about  $85\%$  (as shown in Fig. 1).

IR ( $\text{cm}^{-1}$ ):  $\nu = 3306$  (N-OH),  $\nu = 1645$  (C=N);  $^1\text{H NMR}$  ( $600 \text{ MHz}$ ,  $\text{DMSO-d}_6$ ,  $\delta$ ):  $11.34$  (s, 2H, OH),  $8.18$  (s, 2H, N=C-H),  $7.85$  (s, 1H, Ar-H),  $7.60$  (d, 2H, Ar-H),  $7.44$  (s, 1H, Ar-H);  $^{13}\text{C NMR}$  ( $600 \text{ MHz}$ ,  $\text{CDCl}_3$ ,  $\delta$ ):  $148.26$

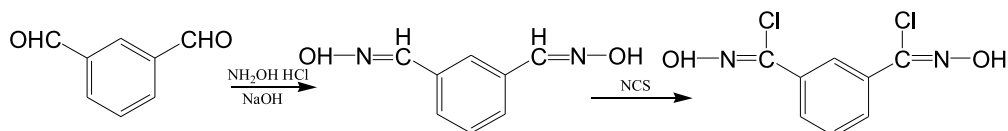


Figure 1. Synthetic route of N,N-dihydroxybenzene-1,3-dicarboximidoyl dichloride

(2C),  $134.02$  (2C),  $129.60$  (1C),  $127.62$  (2C),  $124.68$  (1C); EIMS ( $m/z$ ):  $162.9$  [M-H]<sup>-</sup>. Anal. Calcd for  $\text{C}_8\text{H}_8\text{O}_2\text{N}_2$ : C,  $58.53$ ; N,  $17.06$ ; H,  $4.91$ . Found: C,  $58.71$ ; N,  $17.07$ ; H,  $4.96$ . MP:  $170\sim 172^\circ\text{C}$ .

### Synthesis of N,N-dihydroxybenzene-1,3-dicarboximidoyl dichloride<sup>19</sup>

A solid of N-chlorosuccinimide ( $0.19 \text{ mol}$ ) was added to a solution of benzene-1,3-dicarboxaldehyde dioxime ( $0.08 \text{ mol}$ ) in DMF ( $13 \text{ mL}$ ) with stirring at  $30^\circ\text{C}$ , and progress was monitored by potassium iodide-starch test paper throughout the reaction. Once the reaction was accomplished, the mixture was repeatedly washed with ice water which was extracted by ethyl acetate and dried under vacuum to a constant weight. Finally, the mixture was recrystallized by acetone to give a light yellow solid ( $17.50 \text{ g}$ ), and the yield was about  $93\%$  (as shown in Figure 1).

IR ( $\text{cm}^{-1}$ ):  $\nu = 3231$  (N-OH),  $\nu = 1634$  (C=N),  $\nu = 689$  (C-Cl);  $^1\text{H NMR}$  ( $600 \text{ MHz}$ ,  $\text{DMSO-d}_6$ ,  $\delta$ ):  $12.61$  (s, 2H, OH),  $8.22$  (s, 1H, N=C-H),  $7.91$  (d, 2H, Ar-H),  $7.59$  (s, 1H, Ar-H);  $^{13}\text{C NMR}$  ( $600 \text{ MHz}$ ,  $\text{CDCl}_3$ ,  $\delta$ ):  $162.76$  (2C),  $135.16$  (2C),  $133.55$  (2C),  $129.89$  (1C),  $128.70$  (1C); EIMS ( $m/z$ ):  $232.1$  [M-H]<sup>-</sup>; Anal. Calcd for  $\text{C}_8\text{H}_6\text{O}_2\text{N}_2\text{Cl}_2$ : C,  $41.23$ ; N,  $12.02$ ; H,  $2.59$ . Found: C,  $42.76$ ; N,  $12.55$ ; H,  $3.32$ . MP:  $120\sim 122^\circ\text{C}$ .

### Preparation of polybutadien elastomers

The dichloromethane suspension of N,N-dihydroxybenzene-1,3-dicarboximidoyl dichloride ( $7\%\sim 12\%$ ) and triethylamine (2.1 times) were successively added into a beaker with  $24 \text{ g}$  LPB at low temperature. Herein, N,N-dihydroxybenzene-1,3-dicarboximidoyl dichloride acted as the precursor, and dichloromethane was the solution. After internal bubbles were eliminated at low temperature, the mixture was poured into the teflon

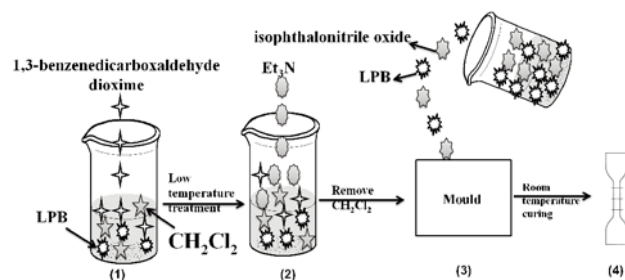


Figure 2. Preparation route of the elastomer

mold (size:  $100 \times 8 \times 2 \text{ mm}^3$ ) for curing in an oven at  $27^\circ\text{C}$  for  $3$  days. The preparation route of the elastomer was shown in Fig. 2.

## RESULTS AND DISCUSSION

### Mechanical Properties

The mechanical behavior of the elastomers added with different amounts of N,N-dihydroxybenzene-1,3-

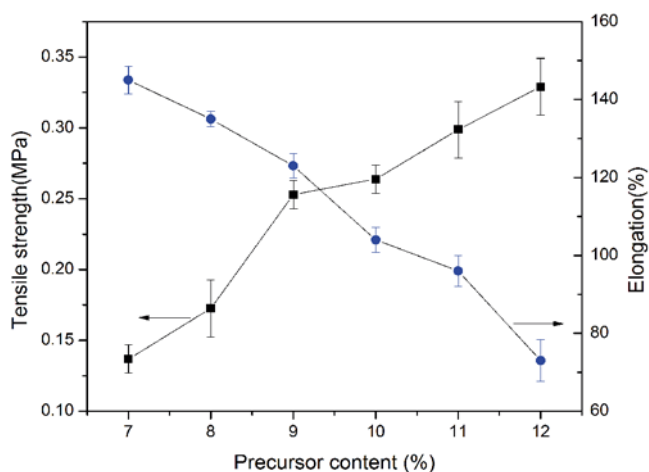


Figure 3. Tensile strength and elongation at break of elastomers

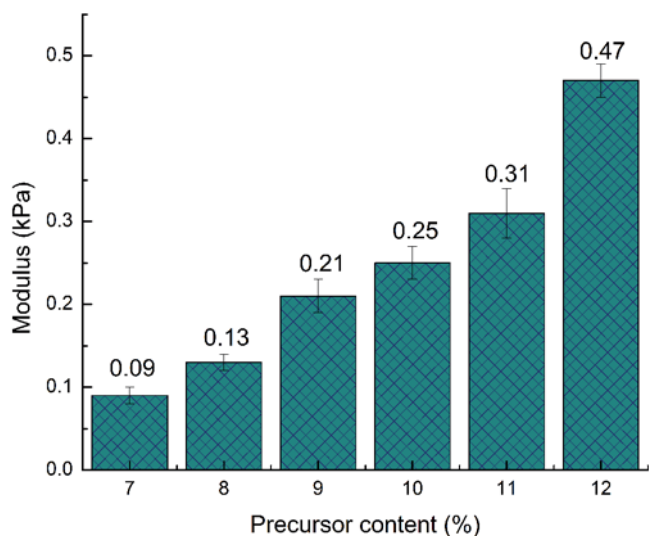


Figure 4. The modulus data of elastomers

-dicarboximidoyl dichloride (precursor) was shown in Fig. 3, Fig. 4 and Fig. 5. When content of the precursor increase, the mechanical properties of elastomers including tensile, modulus and shore hardness are all greatly improved. The crosslinking point of the formed elastomer increased with the content increase of the precursor, and the crosslinking network was compact (as shown in the preparation mechanism of the elastomer in Fig. 6). The tensile strength of the elastomers increased from 0.14 MPa to 0.33 MPa. The curves of elongation at break showed the inverse tendency with increasing tensile strength and modulus of the elastomers, and the

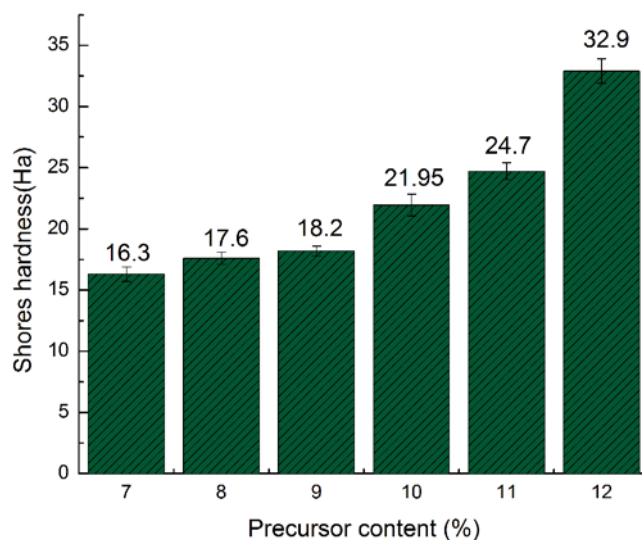


Figure 5. Shore hardness of the elastomers

elongation at break decreased from 145% to 73%. The modulus of the elastomers increased from 0.09 kPa to 0.47 kPa, and the shore hardness of the elastomers increased from 16.3 Ha to 32.9 Ha. In fact, the increasing of cross-linking density often shortens the distance between cross-linking points, which contribute to the inhibition of the segment motion in the elastomers.

It is well known that benzene ring and isoxazoline ring inhibit the free rotation of individual main chain segments, which results in the reduction of chain flexibility<sup>20</sup>, because the hindrance of rotation offered by isoxazoline ring in the elastomers was greater with the increasing of the precursor amounts<sup>21</sup>. As a result, tensile strength and shore hardness for the elastomers become better with the content of the precursor increase. Considering the higher rigidity of polymers chain with increasing benzene ring and isoxazoline ring in elastomers, the modulus of elastomers using polybutadiene as soft segment was investigated<sup>22</sup>. And the results showed higher modulus of the elastomers with the increasing of the precursor amounts.

### Thermal Properties

The glass transition temperature ( $T_g$ ) of elastomers was analyzed by DSC as shown in Fig. 7. It is observed that the  $T_g$  shifted to higher temperature with increasing N,N-dihydroxybenzene-1,3-dicarboximidoyl dichloride. The glass transition temperatures of different systems depend on their own cross-linking density and chain

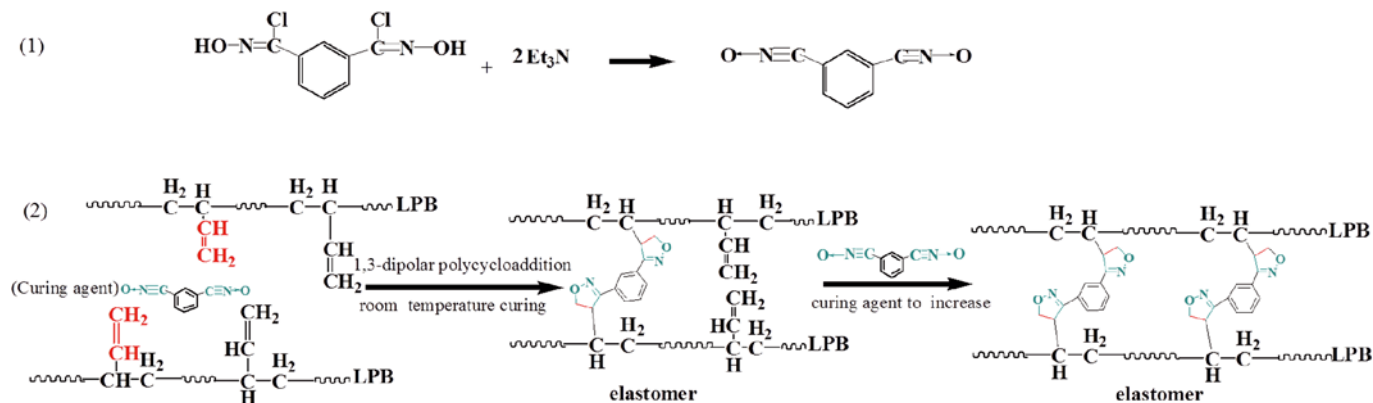
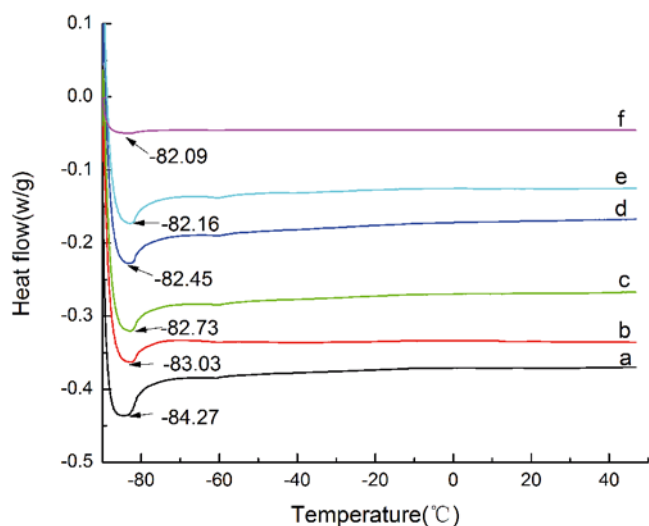


Figure 6. Preparation mechanism of the elastomer

flexible<sup>23</sup>. With the increasing of N,N-dihydroxybenzene-1,3-dicarboximidoyl dichloride, the  $T_g$  values for cross-linking polymers gradually increase from  $-84.27^\circ\text{C}$  to  $-82.09^\circ\text{C}$ , respectively. This behavior can be attributed to lower freedom of movement of the macromolecular segments in the cured state compared to the uncured one<sup>24</sup>. As the chain-length of the cross-linking polymers increases, the cross linking density increased, and thus



**Figure 7.** DSC curves of different elastomers with contents of N,N-dihydroxybenzene-1,3-dicarboximidoyl dichloride: a (7%), b (8%), c (9%), d (10%), e (11%), f (12%)

the free volume within the system reduced resulting in the restrict segment motion of elastomers. Thus, the corresponding  $T_g$  increases.

The thermal stability of the cured elastomers was investigated by TGA. TGA curves of the cured elastomers were given in Fig. 8, and the detailed data were listed in Table 1. Figure 8 shows TGA curves for different elastomers from room temperature ( $25^\circ\text{C}$ ) to  $800^\circ\text{C}$  at a heating rate of  $10^\circ\text{C}/\text{min}$  under  $\text{N}_2$  atmosphere. With the increasing temperature of the curing system, double bonds cross linked in the elastomer. Part of  $\text{C}=\text{C}$  bonds were retained after the 1,3-dipolar cycloaddition of LPB with isophthalonitrile oxides under room temperature. Residual  $\text{C}=\text{C}$  bonds were secondary cured by auto-oxidation in the process of temperature rise. However, the time of secondary curing was longer through self-oxidation mode which was due to the number of double bonds increase. Remained  $\text{C}=\text{C}$  bonds decreased the content increase of curing agent in the elastomer, and the secondary curing was weakened by the auto-oxidation mode. Thus, it can be seen from the figure 8 that when the content of N,N-dihydroxybenzene-1,3-dicarboximidoyl dichloride is 7%, the thermal stability of the elastomer is the best, and which is 12%, the thermal stability of the elastomer is the worst at the same temperature.

The thermal decomposition characteristic of cured elastomer was studied using thermo gravimetric analysis

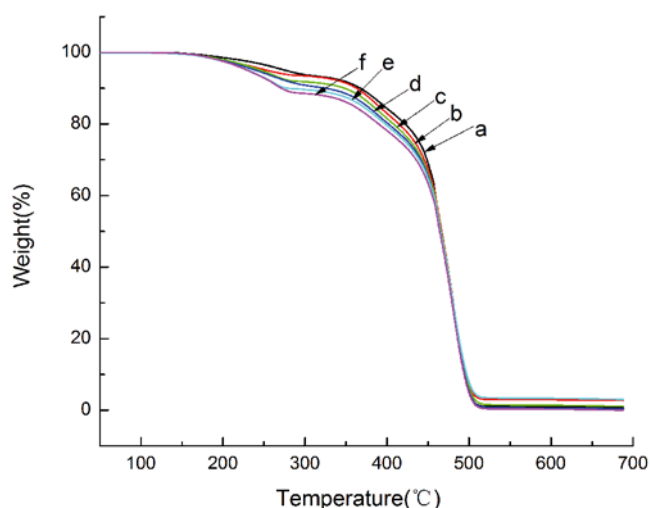


**Figure 8.** TGA curves of different elastomers with contents of N,N-dihydroxybenzene-1,3-dicarboximidoyl dichloride: a (7%), b (8%), c (9%), d (10%), e (11%), f (12%)

(TGA) and the results were compared with different elastomer. All elastomers showed similar thermal degradation behavior with good thermal stability. The first stage decomposition occurs in the temperature range of  $117\sim 295^\circ\text{C}$  with a mass loss of about 7% which was mainly the decomposition of water and small molecules. The second stage decomposition occurs in the temperature range of  $313\sim 407^\circ\text{C}$  with a mass loss of about 10% which was mainly the decomposition of residual  $\text{C}=\text{C}$ . The third stage of the thermal decomposition process was from  $413^\circ\text{C}$  to  $525^\circ\text{C}$ , the cross-linking chain undergoes pyrolysis and combustion, and the elastomers were broken into small molecules after combustion and volatile. And the maximum decomposition temperatures of different elastomers ( $T_{\text{max}}$ , corresponding to a maximum decomposition rate temperature) were all around  $476^\circ\text{C}$ . The cross linking density and the precursor content showed some impacts on the initial decomposition temperature of the elastomers but don't influence their  $T_{\text{max}}$ .

#### FT-IR analysis

In order to observe the cross-linking reaction, IR measurement was conducted on LPB and elastomers. FT-IR provides an efficient way to analyze the curing progress as shown in Fig. 9. The absorption peak of the nitrile group ( $\text{C}\equiv\text{N}$ ) was at around  $2489\text{ cm}^{-1}$  for cured elastomers, which was obviously not observed in LPB. New absorption peaks at  $2680\text{ cm}^{-1}$  correspond to the stretching vibration of the ammonium salt of  $\text{N}^+\text{H}$  in the cured elastomers. New peak at  $1704\text{ cm}^{-1}$  attributed to the absorption of the isoxazoline ring of  $\text{C}=\text{N}$ , indicating the formation of isoxazoline ring during the curing process. The typical absorption peak of the O-H around at  $3006\text{ cm}^{-1}$ ,  $2923\text{ cm}^{-1}$  and  $2848\text{ cm}^{-1}$  was observed in LPB and elastomers. The characteristic peak of the  $\text{C}=\text{C}$  at  $1650\text{ cm}^{-1}$  was observed in the two samples. After the curing reaction was basically completed, the excess nitrile oxide

**Table 1.** The TGA test results of under different curing rate of elastomers

N,N-dihydroxybenzene-1,3-dicarboximidoyl dichloride content %	7	8	9	10	11	12
$T_{5\%}$ [ $^\circ\text{C}$ ]	287	266	258	249	243	242
$T_{10\%}$ [ $^\circ\text{C}$ ]	379	375	360	333	290	283

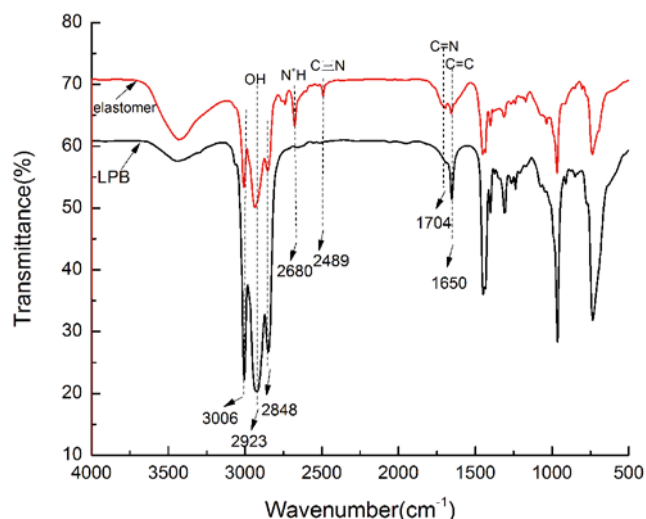


Figure 9. FT-IR spectra of elastomer and LPB

in the elastomer no longer undergoes the dipole ring addition reaction, so the  $C\equiv N$  stretching vibration peak appeared in the elastomer.

### Morphological study

Figure 10 shows SEM images of the elastomers added with different amounts of the *N,N*-dihydroxybenzene-1,3-dicarboximidoyl dichloride (the precursor). SEM technique was used for observing the surface morphology of fracture surfaces in materials. In Fig. 10 (a-d), many smooth tearing ridges and a small number of holes were observed at the fracture surfaces under SEM. Figure 10a shows SEM images of fractured surface morphology of the elastomer exhibiting some relatively smooth tearing ridges at 1,000 times of magnification.

The fracture surface of the elastomer with 8% of the precursor still has smooth edges, though the tearing ridges length of which decrease. As the dosage of the precursor increase to 10%, the length of tearing ridges continues to shorten, and the fracture surface becomes rough as show in fig. 10c-d, which is taken as typical ductile fracture features. Moreover, the fracture of the material is a mixed ductile-brittle fracture, nor it is

a typical brittle fracture or a typical ductile fracture in Fig. 10e. From the images of Fig. 10e, we can see that the brittle fracture of the elastomer (circle ①) is obvious, and circle ② belongs to the ductile fracture at the same resolution. The fracture surface of elastomer in Fig. 10f exhibits a brittle fracture. From Fig. 10f it can be clearly observed that at  $10\mu\text{m}$  resolution, products' burr can be observed in the fracture surfaces of elastomer. A wide range of burr appeared in the elastomer, as shown arrows in Fig. 10f. It was found that, Fig. 10f shows that many tearing ridges of sharp edges were observed at the fracture surfaces of elastomer, indicating that the main fracture mode of elastomer is brittle fracture. Increasing the amount of the precursor in the elastomers resulted in dramatic changes, which were the reduction of ductile fracture and the increase of brittle fracture, in the structure of fracture surfaces.

### Contact angle of the cured elastomer

The different elastomers were cured in a rectangle model with a dimension of  $80 \times 10 \times 5 \text{ mm}^3$  for contact angle measurement as shown in Fig. 11. When the content of the *N,N*-dihydroxybenzene-1,3-dicarboximidoyl

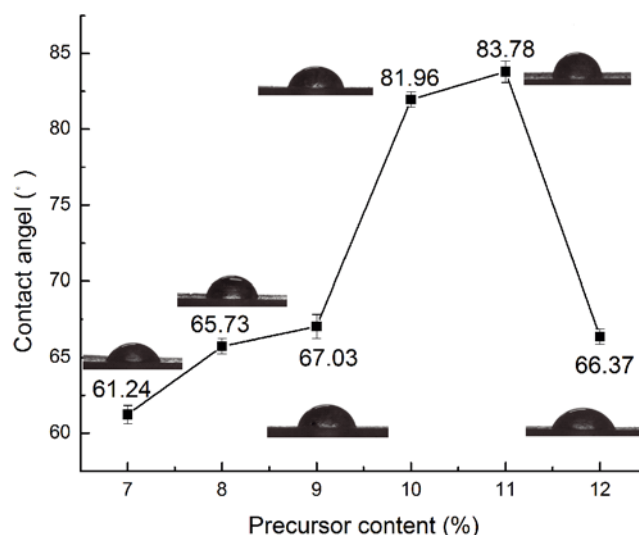


Figure 11. Contact angles of different elastomers

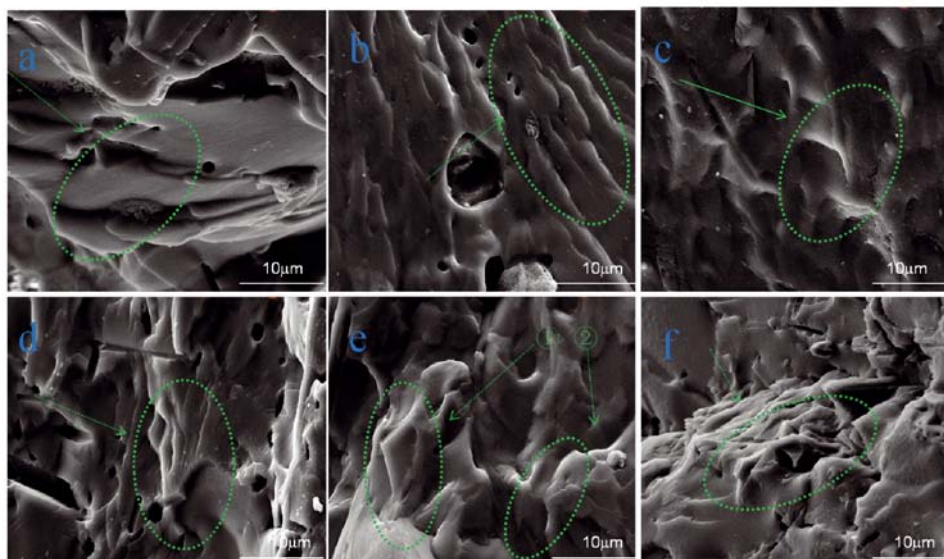


Figure 10. Fracture morphology of different elastomers with contents of *N,N*-dihydroxybenzene-1,3-dicarboximidoyl dichloride: a (7%), b (8%), c (9%), d (10%), e (11%), f (12%)

dichloride increases from 7% to 12%, contact angle increases from 61.24° to 83.78°, then reduces to 66.37°. The highest contact angle is obtained when the addition of the precursor is 11%.

The increase of the contact angle is mainly attributed to the introduction of isoxazoline ring which is hydrophobic into LPB backbones. Isoxazoline ring is a weak polar group, generated from the reaction of 1,3-dipolar cycloaddition of isophthalonitrile oxides and C=C bonds in LPB. The interaction between the surface of the elastomer and water reduces due to the hydrophobic group on the material surface. The amount of isoxazoline increases with the increase of the precursor, leading to the increase in contact angle of the elastomer. However, almost all the C=C double bonds in LPB were consumed when the proportion of the precursor is higher than 11%, giving

rise to only a little increase of isoxazoline ring. Thus, the network structure of the elastomer was completed. Uncured isophthalonitrile oxides began to react through self-polymerization to give a five-membered heterocyclic compound whose exposed oxygen atom forms hydrogen bond with water. The number of hydrogen bonds increases with self-polymerization of isophthalonitrile oxides, as the curing degree of the elastomer increases. As a result, the contact angle of the elastomer decreases with the excess addition of the precursor. Consequently, the elastomer with the optimum hydrophobicity is obtained when the precursor content reaches 11%.

### Effect of heating rate on curing reaction

The kinetics of curing reaction was analyzed by non-isothermal DSC method. The initial temperature  $T_i$ ,

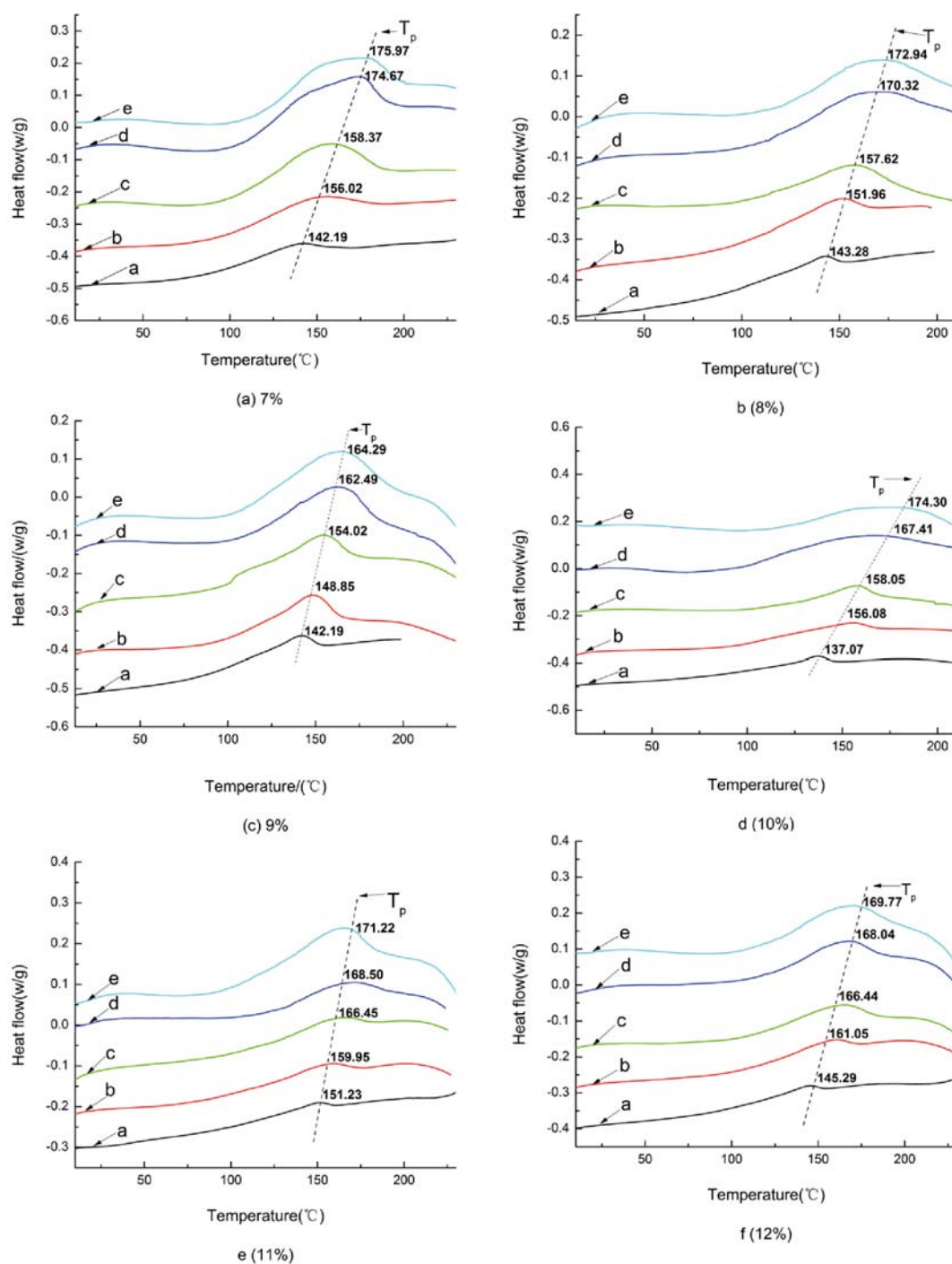


**Figure 12.** DSC curves of elastomers at different heating rates of heating rates: a (5°C/min), b (10°C/min), c (15°C/min), d (20°C/min), e (25°C/min)

peak temperature  $T_p$  and end point  $T_f$  of the curing exothermic peak at different heating rates were obtained from the DSC chart<sup>25</sup>. Figure 12 is the DSC curves of elastomers with the content of the precursor from 7% to 12% at different heating rates. It can be seen that the initial temperature, peak temperature and end point temperature of each curing reaction increases with the increase of the heating rate. During the curing process of elastomers, the thermal inertia and heat flux increased with the heating rate, and the difference in temperature caused by the thermal effect became larger, so the exothermic curing peak shifted to high temperature. At a lower rate of heating, the curing system has sufficient time to react, so the curing reaction of the system could also occur at low temperature. The release of the reaction

heat follows the temperature change, which shows that the curing reaction can be carried out at a relatively low temperature. With the heating rate increasing, the curing of the system was too late to react, the release of heat can not keep up with the temperature changes, and the curing reaction began to happen at higher temperature.

#### Determination of curing process conditions

Curing temperatures of the curing system are different when the heating rate changes, and the peak temperatures are also different during the whole curing reaction process, and then this makes it difficult to determine the curing temperature of the elastomers in the practical curing process. In order to obtain accurate and reliable system characteristic curing temperature, the

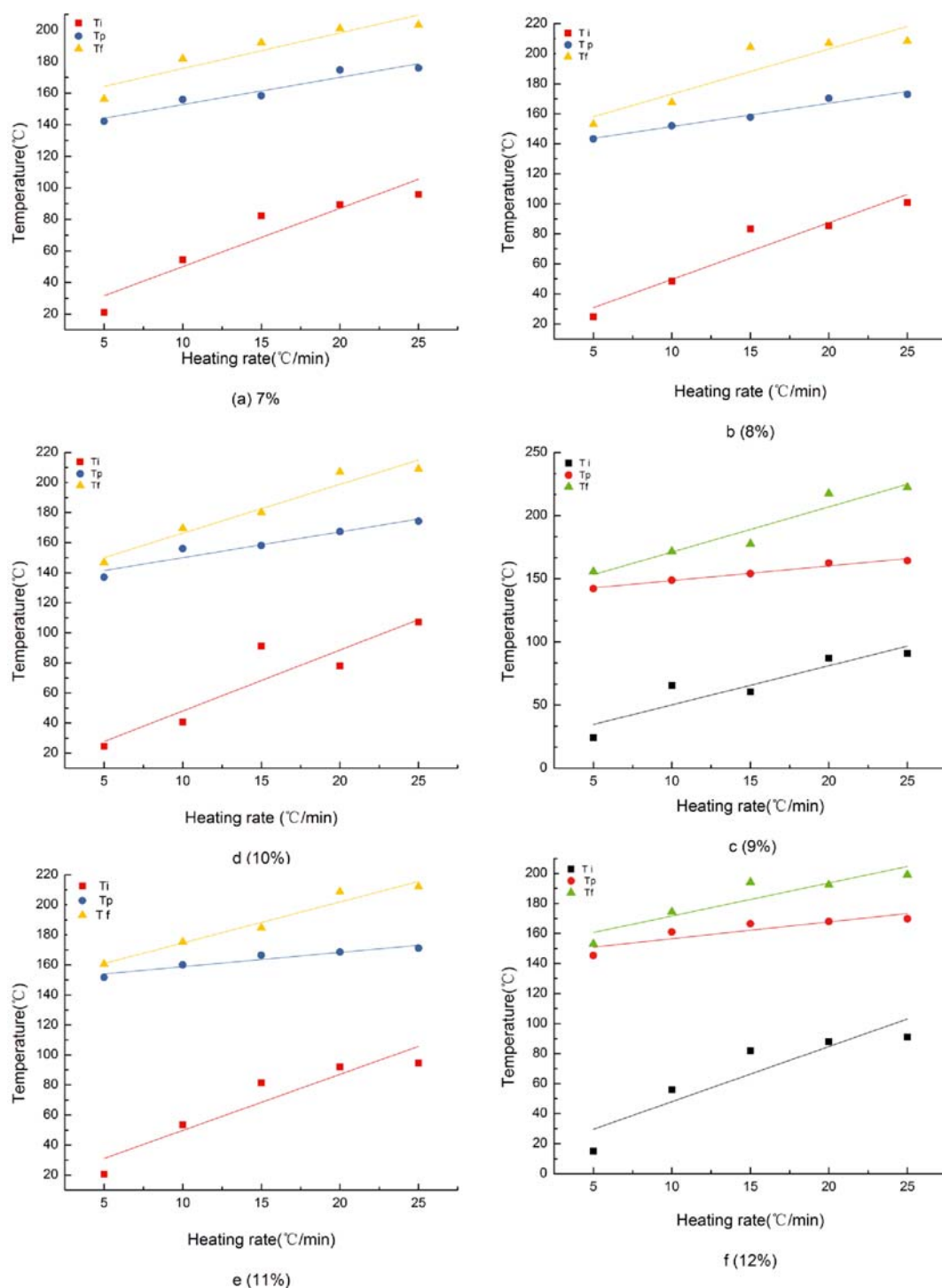


**Figure 13.**  $\beta$ -T curves by extrapolation method with N,N-dihydroxybenzene-1,3-dicarboximidoyl dichloride contents of: a (7%), b (8%), c (9%), d (10%), e (11%), f (12%)

**Table 2.** The curing temperature values of the different curing system

Precursor content of the curing system	Gelation temperature [°C]	Curing temperature [°C]	Post treatment temperature [°C]
7%	13.17	135.58	153.05
8%	11.91	135.92	142.99
9%	11.16	137.02	135.33
10%	12.49	132.85	133.84
11%	12.42	149.25	147.27
12%	11.25	145.32	149.62

T- $\beta$  extrapolation method was used to obtain the curing temperature when the heating rate of  $\beta$  was  $0^\circ\text{C}/\text{min}^{26}$ .

At different heating rates, the initial temperature, peak temperature and termination temperature of the DSC curve of the elastomer were plotted against the heating rate (b) and linearly fitted as shown in Fig. 13. The curing temperature values of different curing systems are shown in table 2. The extrapolation of  $\beta$ -T results indicated that the initial temperature is about  $12.57^\circ\text{C}$ , the peak temperature is about  $139.32^\circ\text{C}$ , and the end point temperature is about  $143.68^\circ\text{C}$  in the elastomer system, respectively. The above temperatures correspond to the gel temperature, curing temperature and post curing temperature in the elastomer system. This indicates that the elastomer has a lower initial curing temperature (the gel temperature). The curing system has higher reactivity with the increase of the temperature. To obtain high performance product the curing system must undergo a post-curing stage. The optimum curing process is as follows: the temperature is raised from the optimum initial curing temperature  $12.07^\circ\text{C}$  to the peak temperature  $139.32^\circ\text{C}$ , and finally raised to the end temperature of  $143.68^\circ\text{C}$  to completely cure the system.

### The kinetic parameters of the curing system

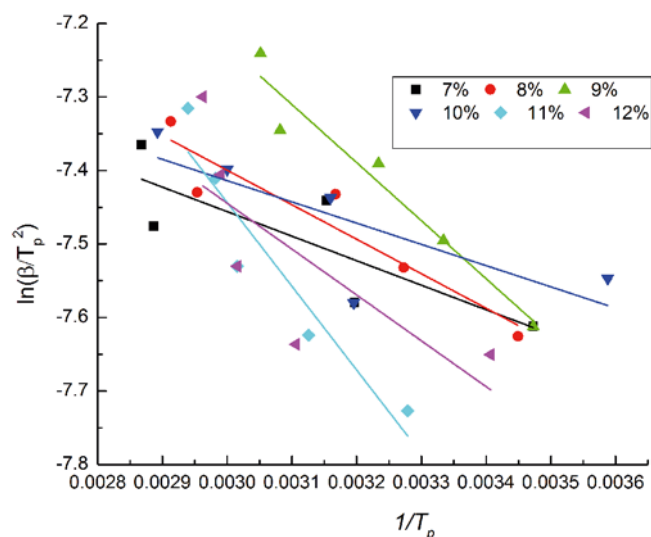
The analysis and calculation of the curing reaction kinetic parameters of the elastomers have an important significance for its application in industry. The value of apparent activation energy ( $E_a$ ) can directly reflect the degree difficulty of the curing reaction in the system. In addition, the parameter of reaction series  $n$  is usually used to describe the complexity degree of the curing reaction system. In this work, Kissinger, Owaza and Crnae equations were used to obtain the linear relation diagrams of  $\ln(\beta/T_p^2)$  and  $\ln\beta$  to  $1/T_p$ , and then the curves were processed by linear fitting method<sup>27-28</sup>. Finally, the values of the apparent activation energy  $E_a$  and the reaction order  $n$  of the system were obtained through the above analysis and calculation.

The apparent activation energy of the curing reaction of the system can be obtained by Kissinger equation as the following equation 1:

$$\frac{d[\ln(\beta/T_p^2)]}{d(1/T_p)} = -\frac{E_a}{R} \quad (1)$$

Where,  $b$  represents the heating rate, K/min;  $T_p$  is the peak temperature, K;  $E_a$  is the apparent activation energy, J/mol;  $R$  is the perfect gas constant with the value of  $8.314 \text{ J}/(\text{mol} \cdot \text{K})$ .

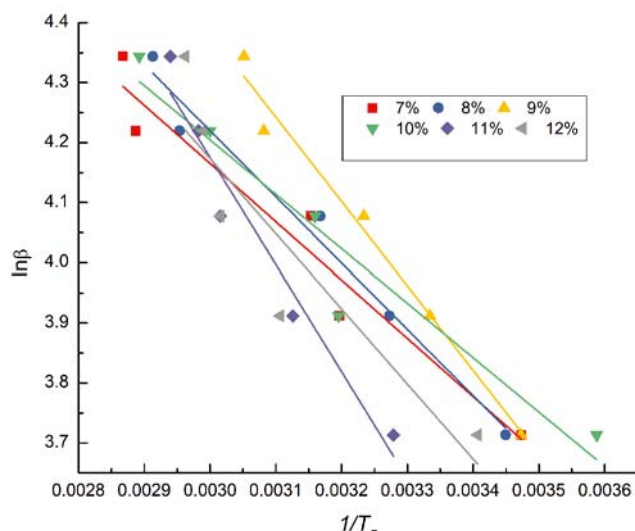
The linear relationship between  $\ln(\beta/T_p^2)$  and  $1/T_p$  can be obtained through Kissinger equation, fitting to

**Figure 14.** The relation between  $\ln(\beta/T_p^2)$  and  $1/T_p$  at Kissinger equation 1

get a straight line, the curve was shown in Fig. 14. The results were calculated in Eq.1 and the value of the apparent activation energy  $E_a$  was obtained.

The apparent activation energy can also be calculated using the Owaza method as the following equation 2:

$$E_a = \frac{-R \cdot \Delta \ln \beta}{1.052 \cdot \Delta(1/T_p)} \quad (2)$$

**Figure 15.** The relation between  $\ln\beta$  and  $1/T_p$  at Owaza equation 2

The parameters in the formula are same as equation 1.

The linear relationship between  $\ln\beta$  and  $1/T_p$  can be obtained through the Owaza equation, fitting to get a straight line, the curve was shown in Fig. 15. The results were calculated in Eq. 2, and the value of the apparent activation energy  $E_a$  was obtained.

According to the relevant researches, the reaction order  $n$  of the curing reduction can be obtained by calculation of the Crnae equation which was shown in Eq. 3. Here, the value of  $E_a/nR$  is much larger than that of  $2T_p$  in the Crnae equation, so Eq. 3 can be simplified into the form of Eq. 4. The linear relationship between  $\ln\beta$  and  $1/T_p$  can be gained through Eq. 2, and the slope of Eq. 4 was obtained by linear fitting to the curve in Fig. 15.

$$\frac{d \ln \beta}{d(1/T_p)} = -(E_a / nR + 2T_p) \quad (3)$$

**Table 3.** The kinetic parameters of curing reaction of elastomers

N,N-dihydroxybenzene-1,3-dicarboximidoyl dichloride content [%]	Apparent activation energy [kJ/mol]		Reaction order
	Kissinger	Ozawa	
7%	8.40	9.48	1.05
8%	8.47	9.16	0.95
9%	8.77	9.71	0.95
10%	8.90	9.88	0.95
11%	9.18	10.08	0.95
12%	9.56	10.10	0.95

$$\frac{d \ln \beta}{d(1/T_p)} = -\frac{E_a}{nR} \quad (4)$$

Table 3 shows the calculated results of apparent activation energy  $E_a$  and reaction order  $n$ . According to the chart, the calculation of activation energy by Kissinger and Ozawa equation were consistent with the law, but in Ozawa equation the activation energy was slightly larger than that in the Kissinger equation. The reaction order was close to 1 and the DSC curve shows a single peak, indicating the curing reaction was similar to the first order reaction, which means that the reaction was easy to proceed.

As can be seen when the content of the N,N-dihydroxybenzene-1,3-dicarboximidoyl dichloride increases there is a systematically increase of apparent activation energy. The 1,3-dipolar cycloaddition reaction of the curing agent and C=C bonds can occur when the energy was greater than  $E_a$  in the curing system. Effective collisions of -CNO of and C=C bonds of decreases with the increase of curing agent in the curing reaction may be caused by the curved structure of LPB chain changes. However, it can be seen from the calculation results that the  $E_a$  of each curing system was less than 10.10 kJ/mol when the content of N,N-dihydroxybenzene-1,3-dicarboximidoyl dichloride was increased from 7% to 12%. The apparent activation energy was low, so the reaction can proceed at room temperature.

## CONCLUSIONS

In order to improve the properties of curing between polymer and nitrile oxide in non-isocyanate curing system, a novel approach aimed at declining the temperature of curing and improving the properties of elastomer was successfully achieved by using of N,N-dihydroxybenzene-1,3-dicarboximidoyl dichloride as the precursor. When the contents of precursor increase, the mechanical properties of elastomer including tensile strength, modulus and shore hardness are all greatly improved. When precursor content of the elastomer increased from 7% to 12%,  $T_g$  only increase by 2.18°C. When the content of the precursor is 11%, the contact angle of the elastomer reaches 83.78° and the hydrophobicity of the elastomer was the best, fracture surface is mainly brittle fracture, these results demonstrates that the curing reaction was basically completed. The kinetic study shows that the curing reaction is a first order reaction, the apparent activation energy increases with the increase of the N,N-dihydroxybenzene-1,3-dicarboximidoyl dichloride.

## ACKNOWLEDGEMENTS

This work was supported by the National Natural Science Foundation of China (51373159) and Equipment Research Foundation of China (61407200202).

## LITERATURE CITED

- Hu, C., Guo, X., Jing, Y., Chen, J., Zhang, C. & Huang, J. (2014). Structure and mechanical properties of crosslinked glycidyl azide polymers via click chemistry as potential binder of solid propellant. *J. Appl. Polym. Sci.* 131 (16), 318–323. DOI: 10.1002/app.40636.
- Lee, D.H., Kim, K.T., Jang, Y., Lee, S., Jeon, H.B. & Paik, H.J., et al. (2014). 1,2,3-triazole crosslinked polymers as binders for solid rocket propellants. *J. Appl. Polym. Sci.* 131 (15), 4401–4404. DOI: 10.1002/app.40594.
- Ajaz, A.G. (1995). Hydroxyl-terminated polybutadiene telechelic polymer (htpb): binder for solid rocket propellants. *Rubber Chem. & Technol.* 68 (3), 481–506.
- Sekkar, V., Alex, A.S., Kumar, V., & Bandyopadhyay, G.G. (2017). Pot life extension of hydroxyl terminated polybutadiene based solid propellant binder system by tailoring the binder polymer microstructure. *J. Macromol. Sci. Part A – Chemistry*, 54 (3), 171–175. DOI: 10.1080/10601325.2017.1265403.
- Cornille, A., Auvergne, R., Figovsky, O., Boutevin, B. & Caillol, S. (2017). A perspective approach to sustainable routes for non-isocyanate polyurethanes. *European Polym. J.* 87, 535–552. <http://dx.doi.org/10.1016/j.eurpolymj.2016.11.027>
- Reshmi, S., Hemanth, H., Gayathri, S. & Nair, C.P.R. (2016). Polyether triazoles: an effective binder for 'green' gas generator solid propellants. *Polymer*, 92, 201–209. <http://dx.doi.org/10.1016/j.polymer.2016.03.006>.
- Krishnan, S.G., KavithaAyyaswamy, & Nayak, S.K. (2013). Hydroxy terminated polybutadiene: chemical modifications and applications. *J. Macromol. Sci. Part A Pure & Applied Chemistry*, 50 (1), 128–138. DOI: 10.1080/10601325.2013.736275.
- Ruechardt, C., Sauer, J. & Sustmann, R. (2005). Rolf huisgen: some highlights of his contributions to organic chemistry. *Cheminform*, 36 (40). DOI: 10.1002/hlca.200590098.
- Sexton, T.M., Freindorf, M., Kraka, E. & Cremer, D. (2016). A reaction valley investigation of the cycloaddition of 1,3-dipoles with the dipolarophiles ethene and acetylene – solution of a mechanistic puzzle. *J. Physical Chem. A*. DOI: 10.1021/acs.jpca.6b07975.
- Binder, W.H. & Sachsenhofer, R. (2010). Polymersome/silica capsules by 'click'-chemistry. *Die Unterrichtspraxis/teaching German*, 29 (12–13), 1097–1103. DOI: 10.1002/marc.200800119.
- Mlostoń, G., Kowalski, M.K., Obijalska, E. & Heimgartner, H. (2017). Efficient synthesis of fluoroalkylated 1,4,2-oxathiazoles via regioselective [3+2]-cycloaddition of fluorinated nitrile oxides with thioketones. *J. Fluor. Chem.* 199: 92–96. <https://doi.org/10.1016/j.jfluchem.2017.04.11>.
- Majumder, S. & Bhuyan, P.J. (2012). Stereoselective synthesis of novel annulated thiopyrano indole derivatives from simple oxindole via intramolecular 1,3-dipolar cycloaddition reactions of nitron and nitrile oxide. *Tetrahedron Lett.* 53 (7), 762–764. DOI: 10.1016/j.tetlet.2011.11.136
- Woodward, R.B. & Hoffmann, R. (1965). Stereochemistry of electrocyclic reactions. *J. Amer. Chem. Soc.* 87 (2), 395–397.
- Breslow D.S., Gardens M. US Patent 3390204 1968.
- Lin, B., Yu, P., He, C.Q. & Houk, K.N. (2016). Origins of regioselectivity in 1,3-dipolar cycloadditions of nitrile oxides with alkynylboronates. *Bioorg. & Medic. Chem.* 24(20), 4787–4790. <https://doi.org/10.1016/j.bmc.2016.07.032>
- Choe, H., Pham, T.T., Lee, J.Y., Latif, M., Park, H. & Kang, Y.K., et al. (2016). Remote stereoinductive intramolecular nitrile oxide cycloaddition: asymmetric total synthesis and structure revision of (-)-11beta-hydroxycurvaralin. *J. Orga. Chem.* 81 (6), 2612 DOI: 10.1021/acs.joc.5b02760.

17. Tegeler, J.J. & Diamond, C.J. (2010). Aroylnitrile oxide cyclizations. 2. synthesis of (3-aroilysoxazol-5-yl)alkanoic acids. *J. Heteroc. Chem.* 24(3), 701–703. DOI: 10.1002/jhet.5570240331.

18. Pan, W., Chen, H., Mu, J., Li, W., Jiang, F. & Weng, G., et al. (2017). Synthesis of high crystalline syndiotactic 1,2-polybutadienes and study on their reinforcing effect on cis-1,4 polybutadiene. *Polymer*, 111, 20–26. <https://doi.org/10.1016/j.polymer.2017.01.022>.

19. Iii, J.B.S., Gardner, D.S., Yao, W., Shi, C., Reddy, P. & Tebben, A.J., et al. (2008). From rigid cyclic templates to conformationally stabilized acyclic scaffolds. part i: the discovery of ccr3 antagonist development candidate bms-639623 with picomolar inhibition potency against eosinophil chemotaxis. *Bioorg. & Medic. Chem. Lett.* 18 (2), 576. <https://doi.org/10.1016/j.bmcl.2007.11.067>

20. Liu, K.C., Shelton, B.R. & Howe, R.K. (1980). A particularly convenient preparation of benzohydroximinoyl chlorides (nitrile oxide precursors). *J. Org. Chem.* 45 (19), 3916–3918.

21. Sugium S, Ueno H, Kono M. US, Patent 3778424 1970.

22. Kissane, M., Lynch, D., Chopra, J., Lawrence, S.E. & Maguire, A.R. (2010). The influence of reaction conditions on the diels-alder cycloadditions of 2-thio-3-chloroacrylamides; investigation of thermal, catalytic and microwave conditions. *Organic & Biomolecular Chemistry*, 8 (24), 5602–5613. DOI: 10.1039/C0OB00368A.

23. Zeng, R.T., Wu, Y., Li, Y.D., Wang, M. & Zeng, J.B. (2017). Curing behavior of epoxidized soybean oil with bio-based dicarboxylic acids. *Polymer Testing*, 57, 281–287. <https://doi.org/10.1016/j.polymertesting.2016.12.007>.

24. Mansilla, M.A., Garraza, A.L.R., Silva, L., Salgueiro, W., Macchi, C. & Marzocca, A.J., et al. (2013). Evolution of the free volume and glass transition temperature with the degree of cure of polybutadiene rubbers. *Polymer Testing*, 32 (4), 686–690. rights reserved. <http://dx.doi.org/10.1016/j.polymertesting.2013.03.001>.

25. Ding, J., Peng, W., Luo, T. & Yu, H. (2016). Study on the curing reaction kinetics of a novel epoxy system. *Rsc Advances*, 7(12). DOI: 10.1039/C6RA25120J.

26. Haddadi, S.A., Kardar, P., Abbasi, F. & Mahdavian, M. (2017). Effects of nano-silica and boron carbide on the curing kinetics of resole resin. *J. Therm. Analysis & Calorimetry*, 128 (2), 1217–1226. DOI: 10.1007/s 10973-016-5951-3.

27. Monteserín, C., Blanco, M., Aranzabe, E., Aranzabe, A. & Vilas, J.L. (2017). Effects of graphene oxide and chemically reduced graphene oxide on the curing kinetics of epoxy amine composites. *J. Appl. Polym. Sci.* 134 (19) 44803. DOI: 10.1002/app.44803.

28. Sharif, M., Pourabbas, B., Sangermano, M., Sadeghi Moghadam, F., Mohammadi, M. & Roppolo, I., et al. (2017). The effect of graphene oxide on uv curing kinetics and properties of su8 nanocomposites. *Polymer International*, 66. 405. DOI: 10.1002/pi.5271.